

Theoretical Study of Dimethyl Maleate and Its Complexes with Lewis Acids: Effect of the Interaction between Two Methoxycarbonyl Groups on Equilibrium Structures

Matsujiro Akakura* **and Nobuaki Koga†**

Department of Chemistry, Aichi University of Education, Igaya-cho, Kariya 448-8542

†Graduate School of Human Informatics, Nagoya University, Chikusa-ku, Nagoya 464-8601

(Received January 30, 2002)

The five equilibrium structures of dimethyl maleate were theoretically determined using the RHF and B3LYP methods. In all of the structures, one of the O=C–O planes is nearly perpendicular to, and the other is coplanar with, the C–C=C–C plane. It is well known that maleic acid diester has peculiar reactivity compared with other conjugated esters, which can be ascribed to the characteristics of the conformations. Calculations of complexes of dimethyl maleate and Lewis acids were performed, and the binding energies for the complexes were analyzed by decomposing them into the deformation energy and the interaction energy. For a comparison, the conformational properties of methyl acrylate and its Lewis acid complexes were also investigated.

Maleic acid diester (maleate) is one of the important compositions in synthesizing polymers as well as organic compounds. There are various polymers in which maleate is used as a monomer unit, because it can be easily introduced into copolymers by radical polymerization.[1] In the field of organic synthesis, maleate is a familiar compound, and it can be modified to the important parts of target molecules, such as prostaglandins, carbacyclin, brefeldin A, and pentalenolactone. The compounds prepared by its Diels–Alder reactions with dienes are often of great value as starting materials for important processes using enzymes.[2]

Recently, Yamamoto and his co-workers have reported on the asymmetric Diels–Alder reactions of nonsymmetrical maleates, and they ascribed the extremely high selectivity to the unique coordination forms of Lewis acids; Et_2AlCl is activated to lead to $AlEt_2^+$, to which both of two carbonyl oxygen atoms of maleate coordinate (maleate–$AlEt_2^+$). They proposed a transition structure in which such an interaction remains.[3]

Several examples of the unique properties of maleate have been confirmed. For instance, it has often been pointed out that maleate has peculiar reactivity compared with other conjugated esters. One example is that dimethyl maleate is much less reactive than dimethyl fumarate in the Diels–Alder reaction. While the reactions of cyclopentadiene with dialkyl fumarates proceeded very fast upon the activation of dialkyl fumarates by bulky monodentate Lewis acid reagents (MAD, MABR), that with dialkyl maleates did not proceed rapidly.[4] Concerning Diels–Alder reaction without a Lewis acid reagent, the reactivities between dialkyl maleate and dialkyl fumarate are different.[5] However, when bidentate Lewis acid reagents, such as $SnCl_4$ and Et_2Al^+, were applied to the reaction of dialkyl maleate, because the Lewis acid reagents activated dialkyl maleate effectively, the reaction took place easily.[4] The other example is that, while a dialkyl fumarate gave homopolymer by radical polymerization, a dialkyl maleate did not homopolymerize at all in the absence of an isomerization catalyst.[6] Why does the reactivity of dialkyl maleate differ from that of dialkyl fumarate? What is the difference between the two similar substances? One possible factor, which would cause these differences, is the interaction between two alkoxycarbonyl groups of maleate, which are located nearby.

In order to elucidate the factors which would realize the peculiarities of dialkyl maleate, we conducted theoretical calculations of the structures and reactivities of dimethyl maleate. Here, as a first part, we report on the results of a theoretical investigation on the equilibrium structures of maleate and its complexes with various Lewis acids. Especially, we focus on the conformations of maleate and the coordination modes of Lewis acid reagents to the carbonyl oxygen of maleate. In theoretical calculations, we adopted the RHF and B3LYP methods, as mentioned in computational methods. The shown results are at the B3LYP level, unless otherwise noted.

We hope that the data given in this paper could give a basic idea of chemistry concerning multi-functional groups, like polymer chemistry, organic chemistry, supermolecular chemistry, and biochemistry.

Results and Discussion

Dimethyl Maleate. Calculations at the RHF levels have been carried out to determine the equilibrium structures of possible conformers of dimethyl maleate. As shown in Fig. 1 we obtained five equilibrium structures in which one of the O=C–O planes is nearly perpendicular to the C–C=C–C plane, and the other is coplanar with the same C–C=C–C plane. From now on, we express the conformations of dimethyl maleate with three letters, as can be seen in Fig. 1. The first two letters denote the conformations of perpendicular and in-plane

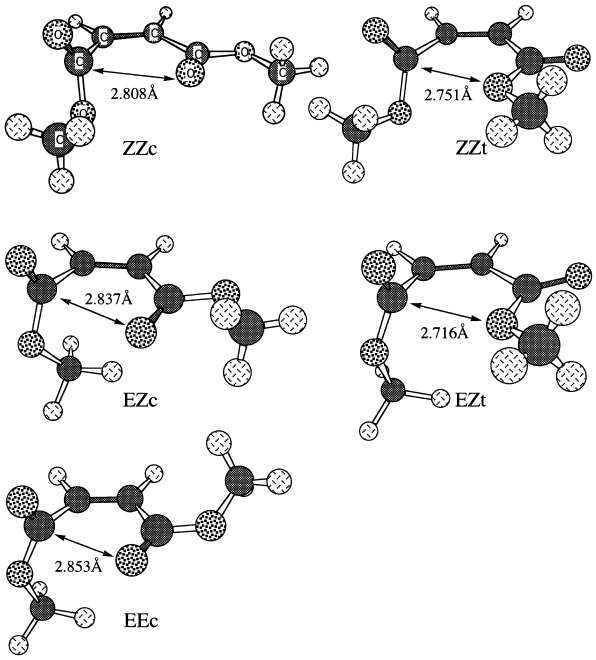

Fig. 1. RHF/6-31G* optimized structures of dimethyl maleate. B3LYP/6-31G* structures are similar. See Table 1.

$COOCH_3$ groups, with "Z" and "E" indicating (*Z*)- and (*E*)-conformation, respectively. Because the last letter designates the conformation of a nearly coplanar C=C–C=O skeleton, "c" and "t" indicate *s-cis* and *s-trans* conformations, respectively. Because of these conformation possibilities there are eight possible conformers. In reality, we started geometry optimizations with the structures of eight possible conformers to eventually obtain the five structures shown in Fig. 1. Calculations starting with the ZEc, ZEt, and EEt conformers resulted in one of the structures in Fig. 1. For instance, when the geometry determination was started from the ZEc structure, which was created by changing the conformation of the optimized EEc structure, we obtained the EZt conformer. We also started geometry optimizations from structures with two in-plane $COOCH_3$ groups to obtain the structures shown in Fig. 1. Thus, we could conclude that there are only five equilibrium structures on the potential energy surface for dimethyl maleate.

In order to obtain further insight into the conformation behavior, we calculated at the RHF level the potential energy curve for the O^1=C–C=C torsion while fixing the C–C=C–C=O^2 skeleton to be planar and optimizing the structures at every 15° of the O^1=C–C=C torsion angle. The thus-obtained O^1=C–C=C torsion potential energy curve is shown in Fig. 2. One can find that there is only one minimum at the O^1=C–C=C dihedral angle of 105° which corresponds to ZZt. This supports the above results about the conformation in the equilibrium structures.

The fact that ZEt and EEt structures are not equilibrium structures is obviously due to the steric repulsion between the perpendicular $COOCH_3$ group and the CH_3 group of the in-plane $COOCH_3$ group.

The relative energies of the five conformers calculated at the B3LYP and RHF levels are compared in Table 1. The B3LYP results show the same tendencies as the RHF results. The results given in Table 1 show that the ZZc conformer is the most stable. One can note that, concerneing the conformation of the $COOCH_3$ groups, (*Z*)-conformer is more stable than (*E*)-conformer (Chart 1) and that the energy difference between them is 6.2 and 8.6 kcal mol^{-1} for the perpendicular and in-plane $COOCH_3$ groups, respectively. The stability of (*Z*)-conformation can be explained in terms of i) the interaction between the lone pair of OCH_3 and the σ^* orbital of C=O[7], and ii) the electrostatic interaction between the local dipole moments,[8] as shown below. The electron repulsion between the lone pairs of OCH_3 and C=O in (*E*)-conformation is another factor destabilizing (*E*)-conformer.

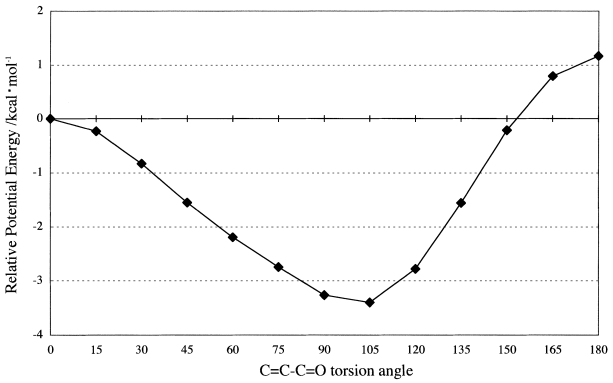

Fig. 2. Potential energy curve for C=C–C=O torsion in dimethyl maleate calculated at the RHF/6-31G* level. The two $COOCH_3$ groups have the (*Z*)-conformation, and the minimum corresponds to the ZZt conformer.

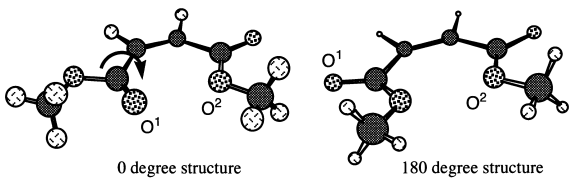

Table 1. Energies of Dimethyl Maleate in kcal mol^{-1} Relative to the Most Stable ZZc Comformer[a)]

	RHF/6-31G*	B3LYP/6-31G*
ZZc	0.00	0.00
ZZt	1.07	1.06
EZc	8.28	6.26
EZt	8.84	7.30
EEc	18.19	14.83

a) All the structures were optimized at the respective level.

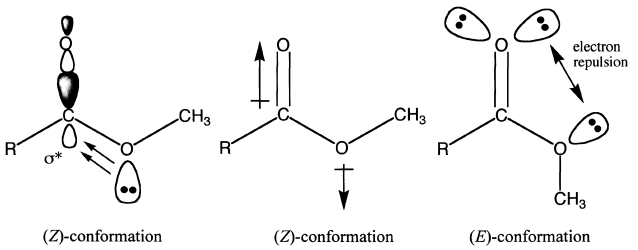

Chart 1.

Fig. 3. RHF/6-31G* optimized structures of [a] C_2H_5-COCH=CHCOOCH$_3$ and [b] $CH_3O(CH_2=)CCH=CHCO$-OCH$_3$.

The (*E*)-(*Z*) energy difference for the perpendicular COOCH$_3$ group is similar to that in methyl formate (5.3 kcal mol^{-1}), whereas that for the in-plane COOCH$_3$ group is close to that in methyl acrylate (8.9 kcal mol^{-1}, see below). In other words, it seems reasonable to suppose that the –CH=CH–COOCH$_3$ moiety in dimethyl maleate behaves almost independently of the –COOCH$_3$ moiety.

Changing the conformation of ZZc from *s-cis* to *s-trans* leads to a 1.1 kcal mol^{-1} less stable ZZt conformer. The tendency that the *s-cis* conformer is more stable than the *s-trans* conformer will be shown in the case of methyl acrylate as well (see "Methyl Acrylate" section).

Why is one of the COOCH$_3$ groups out of the C–C=C–C plane, although it causes π conjugation stability to be lost? In order to answer this question, we determined the structures by replacing the methoxy group of the perpendicular COOCH$_3$ group by an ethyl group, or by substituting the carbonyl oxygen atom of the same COOCH$_3$ group by methylene. The thus-obtained structures are shown in Fig. 3.

One can notice that the conformational behavior is completely different between these two model compounds. In the former model compound, the COCH$_2$CH$_3$ group is still perpendicular. On the other hand, the COOCH$_3$ and C(=CH$_2$)OCH$_3$ groups in the latter model compound show a much smaller deviation from planarity. These results suggest that the interaction between the carbonyl π* orbital of the perpendicular COOCH$_3$ group and the carbonyl oxygen lone pair of the in-plane COOCH$_3$ group (n–π* interaction shown below)[9] is responsible for the structural feature that one of the COOCH$_3$ groups is perpendicular in dimethyl maleate.

As a matter of fact, the Mulliken overlap population shown below (0.032) indicates that there is a bonding interaction (Chart 2).

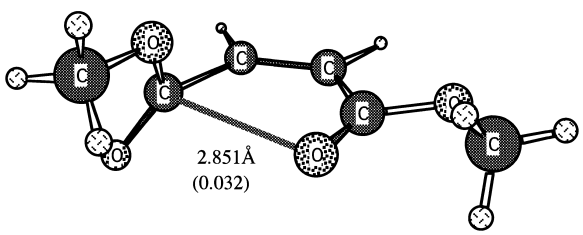

Chart 2.

As shown below, the energy differences between the perpendicular and planar structures for methyl acrylate and 2-methoxy-1,3-butadiene were calculated at the RHF/6-31G* level. The calculations show that the conjugation between the C=C and C=O bonds is stronger than that between the C=C bonds, suggesting that, although the strong conjugation is lost, the n–π* interaction covers the loss in the conjugation energy and prefers the perpendicular structure (Chart 3).

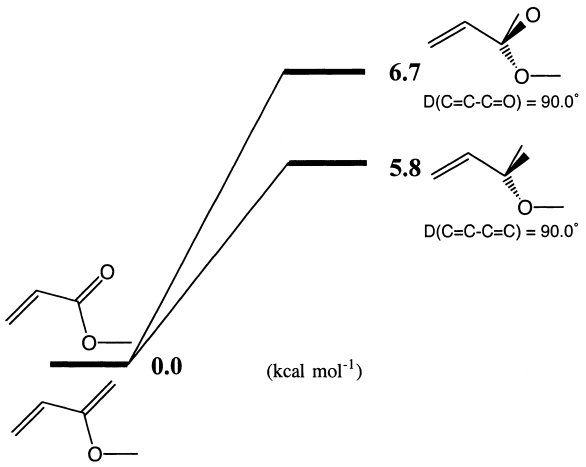

Chart 3.

The norbornene derivative with two COOCH$_3$ groups, the product of Diels–Alder reaction of dimethyl maleate with cyclopentadiene, also has a structure in which n–π* interaction takes place (Fig. 4).

Methyl Acrylate. Since the above results show that dimethyl maleate consists of the "methyl formate" (–COOCH$_3$) and "methyl acrylate" (–CH=CH–COOCH$_3$) moieties, a comparison of the conformational properties between dimethyl maleate and methyl acrylate is expected to give further insight. Therefore, we determined the structures of the four plausible conformers of methyl acrylate at the B3LYP level, as shown in Fig. 5. They are denoted by Zc, Zt, Ec, and Et, in which the first character, "Z" or "E", designates the conformation of the COOCH$_3$ group and "c" and "t" indicate *s-cis* and *s-trans* conformations of the C=C–C=O skeleton, respectively. The C=C and C=O bonds in the optimized structures of (*Z*)-conformation are almost coplanar (Fig. 5). In order to verify that there is no other energy minimum in changing the C=C–C=O torsion

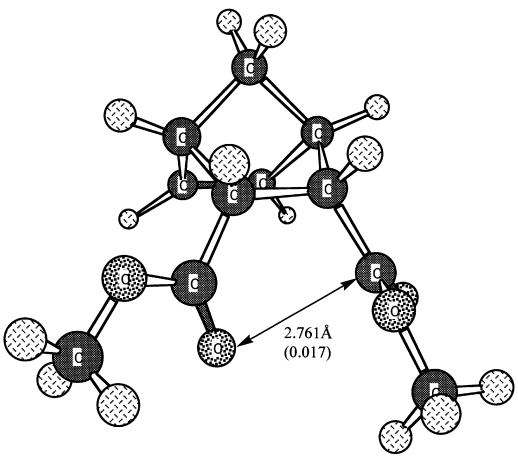

Fig. 4. RHF/6-31G* optimized structure of the Diels–Alder product of dimethyl maleate and cyclopentadiene. [(5*R*,6*S*)-5,6-bis(methoxycarbonyl)-2-norbornene].

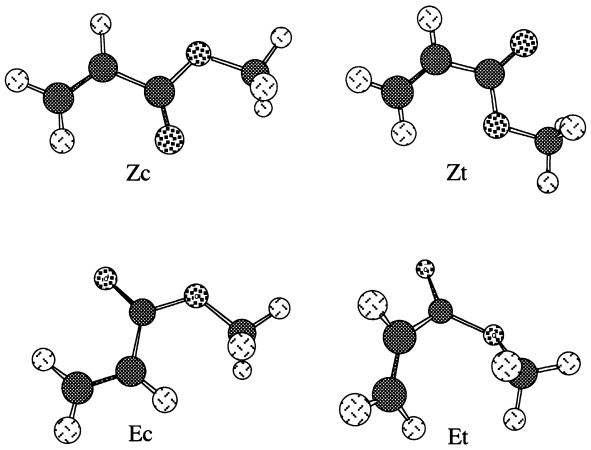

Fig. 5. Optimized structures of methyl acrylate. RHF and B3LYP methods gave the qualitatively same structures.

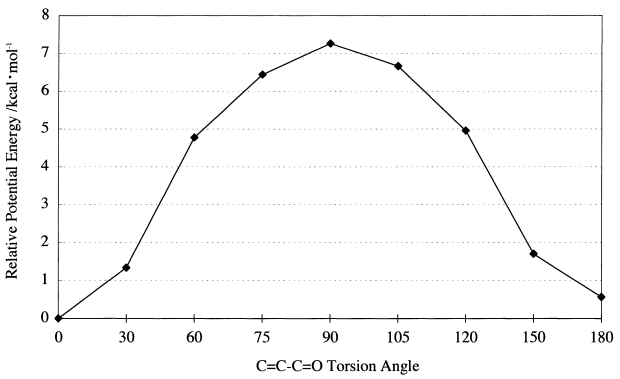

Fig. 6. Potential energy, curve for C=C–C=O torsion of methyl acrylate calculated at the RHF/6-31G* level. The $COOCH_3$ group has the (*Z*)-conformation.

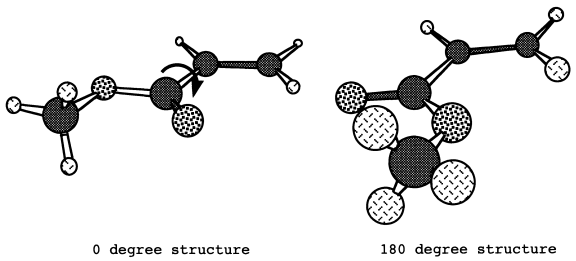

angle, we calculated at the RHF level the potential energy curve while changing the C=C–C=O torsion angle of the (*Z*)-conformer and optimizing the other structural parameters (Fig. 6). The thus-obtained curve has no other energy minimum; the maximum is at 90°. This energy increase is apparently due to a loss of stabilization by C=C–C=O conjugation (7.3 kcal mol^{-1} relative to the *s-cis* conformation at the RHF level). The relative energies of the conformers are summarized in Table 2, in which the MP4 relative energies calculated for the B3LYP structures are also shown. One can find that both levels of calculation give quite similar results.

It is first noted that the (*Z*)-conformers are much more stable than the (*E*)-conformers, in agreement with the above discussion for dimethyl maleate; Zc and Zt are more stable than Ec and Et by 8.9 and 11.5 kcal mol^{-1}, respectively, at the B3LYP level. These values are larger than that for methyl formate (5.3 kcal mol^{-1}), indicating that the C=C–C=O conjugation affects the (*E*)–(*Z*) energy difference by a few kcal mol^{-1}.

Table 2. Energies of Methyl Acrylate in kcal mol^{-1} Relative to the Most Stable Zc Comformer

	B3LYP/6-31G*	MP4/6-31G* a)
Zc	0.00	0.00
Zt	0.72	0.84
Ec	8.87	9.77
Et	12.24	12.55

a) Calculated at the B3LYP/6-31G* optimized structures.

The energy difference between *s-cis* and *s-trans* is much smaller; Zc is more stable than Zt by 0.7 kcal mol^{-1}. The larger energy difference of 1.1 kcal mol^{-1} between ZZc and ZZt of dimethyl maleate can be ascribed to the n–π^* interaction between the two $COOCH_3$ groups mentioned above. On the other hand, Ec is more stable than Et by 3.4 kcal mol^{-1}, and this larger value can be ascribed to the large steric repulsion between the methylene hydrogen and the CH_3 group in Et (Chart 4). The Mulliken overlap population indicates a weak-bonding interaction between the methylene hydrogen and the methoxy or carbonyl oxygen atoms in the Zc-, Zt-, and Ec-forms (Zc: 0.023, Zt: 0.019, Ec: 0.028, Et: 0.005). Interestingly the overlap populations in the case of carbonyl oxygen are slightly bigger than those in the case of methoxy oxygen. This difference may be one of the factors favoring the *s-cis* conformation. Fausto et al. proposed that the factors which determine the relative stability of the *s-cis* and *s-trans* conformers are a mesmerism favoring the *s-cis* conformer, the steric repulsion between the vinyl group and the methoxy oxygen atom in the *s-trans* conformer,[10] and the large attractive bond dipole interaction in the *s-cis* conformer.[10]

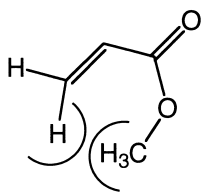

Et conformation

Chart 4.

The results for methyl acrylate given in this chapter show that this molecule has a planar structure, and that the (*Z*)-conformer is more stable than the (*E*)-conformer. They are the trends found in the "methyl acrylate" moiety of dimethyl maleate, supporting the idea that dimethyl maleate consists of the "methyl acrylate" and "methyl formate" moieties.

Dimethyl Maleate–AlH_3 Complexes. Next, we studied the structures of Lewis acid complexes of dimethyl maleate, in which AlH_3 was adopted as a model of a Lewis acid. Four modes of AlH_3 coordination to dimethyl maleate are possible, as shown in Fig. 7 for ZZc as an example. "**I**" and "**II**" in the structure's names in Fig. 7 mean that AlH_3 coordinates to dimethyl maleate at the carbonyl oxygen of the *perpendicular* $COOCH_3$ group from the anti and syn sides relative to the

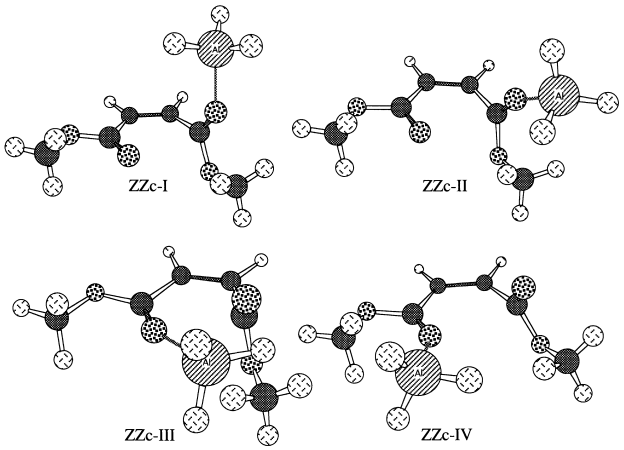

Fig. 7. RHF/6-31G* optimized structures of dimethyl maleate–AlH_3 complexes

methoxy group, respectively. "**III**" and "**IV**" designate the coordination of AlH_3 to a carbonyl oxygen of the conjugated, *in-plane* $COOCH_3$ group from the anti and syn sides, respectively. Because we found five structures for isolated dimethyl maleate, there are twenty possible complexes. Since we have so many possible structures, we adopted the following strategy to save CPU time: first, we determined the structures at the RHF level to select relatively stable ones; we then optimized the structures of selected conformers at the more reliable B3LYP level. The energies of the conformers are compared in Table 3. A comparison of the energies among those complexes with the same AlH_3 coordination modes shows that the trend in stability reflects that of isolated dimethyl maleate; for instance, ZZc-I is more stable than other type **I** complexes, such as ZZt-I and EZc-I.

Table 3. Energies of Dimethyl Maleate–AlH_3 Complexes in kcal mol^{-1} Relative to the Most Stable ZZc-I Structure[a)]

	RHF/6-31G*	B3LYP/6-31G*
ZZc-I	0.00	0.00
ZZc-II	2.84	2.96
ZZc-III	ZZc-IV[b)]	ZZc-IV[b)]
ZZc-IV	3.24	2.51
ZZt-I	1.97	1.59
ZZt-II	3.80	ZZc-IV[b)]
ZZt-III	ZZc-I[b)]	ZZt-I[b)]
ZZt-IV	4.22	4.16
EZc-I	7.31	5.64
EZc-II	8.60	7.00
EZc-III	EZc-IV[b)]	
EZc-IV	13.03	
EZt-I	8.83	7.63
EZt-II	8.60	7.61
EZt-III	10.60	
EZt-IV	12.62	
EEc-I	16.33	13.22
EEc-II	19.07	16.01
EEc-III	EEc-IV[b)]	
EEc-IV	19.91	

a) All the structures were optimized at the respective level. b) Geometry optimization gave the different structure shown.

The calculations showed that **I** is the most stable among those complexes with the same conformation of dimethyl maleate and that **II** is the next, except for the EZt-form. For the EZt-form, the energies of **I** and **II** are almost degenerate. The type-**III** conformation is unstable, and the geometry optimizations converged to the other forms, except in the case of the EZt-form. This is presumably because of the steric repulsion between AlH_3 and the perpendicular $COOCH_3$ group. Though we could determine the structures of coordination mode **IV** for all conformations of dimethyl maleate, they are the least stable structures among those which we could determine. Thus, not only the conformations of dimethyl maleate, but also the coordination modes of AlH_3 influence the stability of the complexes. As a result, ZZc-I is the most stable.

The energy difference between **II** and **I** was calculated at the B3LYP level to be 3.0 kcal mol^{-1} for ZZc and 1.4 kcal mol^{-1} for EZc, indicating that the difference in the steric environment between the anti and syn coordination to the (*E*)-$COOCH_3$ group is smaller. For EZt, the difference in energy (-0.02 kcal mol^{-1} at the B3LYP level) between **I** and **II** is thus very small.

It was observed in this section that AlH_3 is more proper to coordinate to the carbonyl oxygen of the *perpendicular* $COOCH_3$ group than that of the *in-plane* $COOCH_3$ group in dimethyl maleate.

Methyl Acrylate-AlH_3 and Methyl Acrylate-BF_3 Complexes. For a comparison we studied the AlH_3 complex of methyl acrylate. Since there are four conformers of methyl acrylate, and we have two possible coordination modes of a Lewis acid to a carbonyl oxygen, syn and anti with respect to the methoxy group, there are totally eight possible conformers of the AlH_3 complex as shown in Fig. 8. As a matter of fact, the structures of all the conformers were successfully determined, as shown in Table 4. It was found that the most stable is the Zt-anti conformer, which has the (*Z*)-conformation of $COOCH_3$ group, *s-trans* conformation about the C=C–C=O skeleton, and the AlH_3 coordination from the anti side relative to the methoxy group. Because the crystal structure of the $SnCl_4$/ethyl cinnamate complex[11] has been experimentally shown to have conformations corresponding to Zt-anti, such conformations have been believed to also be favorable in solution. The results obtained here will give further support of this belief.

Also, one can note that the (*Z*)-conformers are more stable than the (*E*)-conformers, reflecting the stability order of isolated methyl acrylate shown in Table 2. The energy difference between anti- and syn-coordination for the Zc and Et conformers is smaller than that for the Zt and Ec conformers. The steric difference between the anti- and syn-coordination is smaller in the cases of the Zc and Et conformers. On the other hand, obviously, the *syn*-coordination to the Zt conformer is more crowded than the anti-coordination, and the *anti*-coordination to the Ec conformer is sterically less favorable than the syn-coordination.

Dimethyl Maleate-$TiCl_4$ Complexes. Next, we studied the complexes of dimethyl maleate with the Lewis acid of $TiCl_4$, which can have two additional coordination sites, in order to investigate whether a chelate complex exists. Different

Table 4. Energies of Methyl Acrylate–BF3 and –AlH_3 Complexes in kcal mol^{-1} Relative to the Most Stable Conformer[a)]

	AlH_3		BF_3	
	RHF/6-31G*[b)]	B3LYP/6-31G*	RHF/6-31G*	B3LYP/6-31G*
Zc-anti		0.37	1.93	1.44
Zc-syn		1.40	1.51	1.95
Zt-anti	0.00	0.00	0.00	0.00
Zt-syn	1.89	2.36	1.51	2.95
Ec-anti		8.80	12.45	10.66
Ec-syn		7.46	9.46	9.06
Et-anti		12.68	15.86	13.17
Et-syn		12.25	15.60	13.83

a) All the structures were optimized at the respective level. b) The calculations were carried out for Zt-anti and Zt-syn only.

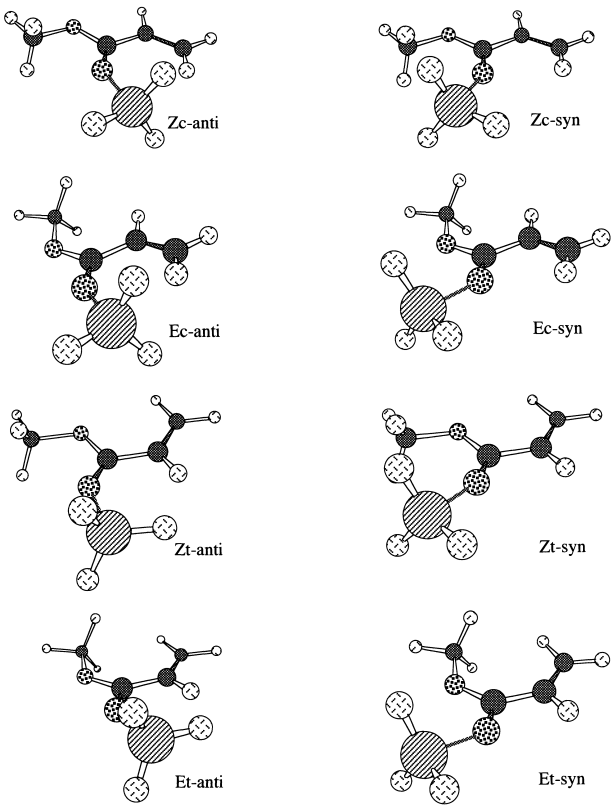

Fig. 8. Optimized structures of methyl acrylate–AlH_3 complexes. RHF and B3LYP methods gave the qualitatively same structures.

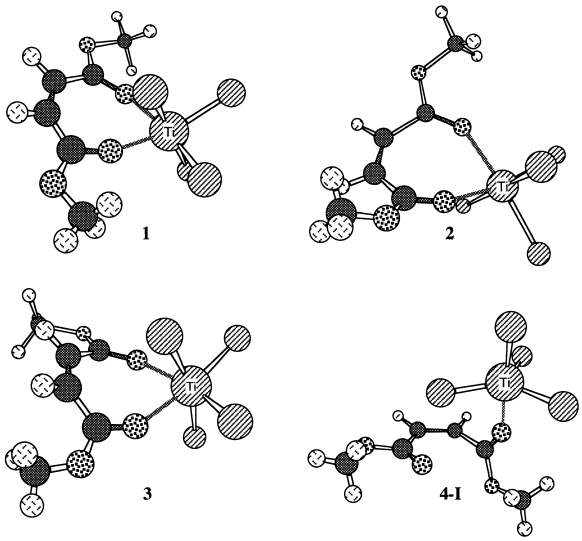

Fig. 9. RHF/6-31G* optimized structures of dimethyl maleate–$TiCl_4$ complexes.

Table 5. Energies of Dimethyl Maleate–$TiCl_4$ Complexes in kcal mol^{-1} Relative to the Most Stable Conformer[a)]

	RHF/6-31G*	B3LYP/6-31G*
1	0.00	0.00
2	12.83	
3	25.80	
4-I	5.42	2.61
4-II	**4-I**[b)]	
4-III	—[c)]	
4-IV	**4-I**[b)]	

a) All the structures were optimized at the respective level. b) Geometry optimization gave the different structure shown. c) Geometry optimization was not investigated.

from the AlH_3 and BF_3 complexes, we found the chelate structures as well as the non-chelate structures for $TiCl_4$ complexes at the RHF level. The thus-obtained structures are summarized in Fig. 9, and the relative energies are given in Table 5. As shown in Fig. 9, we found three chelate complexes: **1**, **2**, and **3**. Since in these structures the two $COOCH_3$ groups coordinate to the Ti atom, we call them (Zc-anti, Zc-anti), (Ec-anti, Zc-anti), and (Ec-anti, Ec-anti), respectively, combining the notations used in the cases of methyl acrylate–Lewis acid complexes.

The results given in Table 5 show that **1** is the most stable, reflecting the preference of (*Z*)-conformation. Changing the conformation of one $COOCH_3$ group in **1** from (*Z*) to (*E*) leads to 12.8 kcal mol^{-1} less stable **2**. If the conformation of the other $COOCH_3$ group in **2** is also changed from (*Z*) to (*E*), **3** is given which is 13.0 kcal mol^{-1} less stable than **2**. These energy increases in changing the conformation of a single $COOCH_3$ group are reasonably close to that for the methyl acrylate-BF_3 complex (10.5 kcal mol^{-1} at the RHF level).

Concerning non-chelation complexes we investigated the complexation of $TiCl_4$ to the ZZc form of dimethyl maleate, because such complexes are relatively stable, as discussed above concerning AlH_3 complexes. When geometry optimizations were started with structures called **4-I**, **4-II**, and **4-IV**, which correspond to ZZc-I, ZZc-II, and ZZc-IV shown in Fig. 7 for the AlH_3 complexes, all of the geometry optimizations converged to **4-I**, presumably because the bulky $TiCl_4$ favors the least-crowded site. **4-III**, which corresponds to ZZc-III in Fig. 7, was not investigated, because , as shown in the case of the AlH_3 complex, it would be unstable.

We thus determined at the B3LYP level the structures of **1** and **4-I**, as shown in Table 5. The calculations showed that the chelation form **1** is lower in energy than the complex in the non-chelation form **4-I** by 5.4 kcal mol^{-1} at the RHF level and 2.6 kcal mol^{-1} at the B3LYP level. Since the chelation form is tighter, the entropy would make it less favorable. A comparison of the free energy, which was calculated using the non-scaled vibrational frequencies, showed the stability order of the chelate and non-chelate structures is unchanged; the chelate form is more stable at 298.15 K (RHF: 3.4 kcal mol^{-1}, B3LYP: 1.7 kcal mol^{-1}). Consequently, it can be concluded that the complex of dimethyl maleate with $TiCl_4$ takes chelate coordination mode.

Complexes of Dimethyl Maleate with Other Lewis Acids. The calculations made so far have shown that the Lewis acids of the main elements favor non-chelation coordination, whereas $TiCl_4$ bridges the two carbonyl oxygen atoms, in which the Ti atom takes six-coordination. This suggests that if two or more vacant coordination sites are available on the metal atoms of a Lewis acid, a chelation structure would be realized. We thus performed calculations with other various Lewis acids: BCl_3, AlH_2^+, $AlMe_2^+$, $AlMe_3$, SnH_4, and $SnCl_4$. The obtained structures are summarized in Table 6 together with the above results. While the Lewis acids possessing only one vacant orbital (AlH_3, $AlMe_3$, BF_3, and BCl_3) form non-chelate complexes, those with two vacant orbitals on the metal center (AlH_2^+, $AlMe_2^+$) form, as expected, chelate complexes with dimethyl maleate. If the coordination number of the central metal atoms could increase by one or more, chelate structures would be possible. $TiCl_4$ and $SnCl_4$ are two cases. In the latter case, the Sn atom becomes hypercoordinated. On the other hand, in the case of SnH_4, this hydride is not sufficiently acidic to form the complex, and therefore it dissociates from dimethyl maleate, resulting in the formation of a weak complex.

Table 6. The Most Stable Structures of Dimethyl Maleate–Lewis Acid Complexes

	B3LYP/6-31G*
BF_3	ZZc-I type
BCl_3	ZZc-I type[a)]
AlH_2^+	ZZ(chelate) type
$AlMe_2^+$	ZZ(chelate) type
AlH_3	ZZc-I
$AlMe_3$	ZZc-I type
$AlCl_3$	ZZc-I type
$TiCl_4$	**1**[a)]
SnH_4	a weak complex[a)]
$SnCl_4$	**1** type[a)]

a) Only RHF geometry determination was performed.

The results of calculations with AlR_2^+ are in agreement with the experimental consideration by Yamamoto and his coworkers[3] mentioned in the Introduction. On the other hand, Maruoka et al. have recently proposed a bidentate coordination of α-methoxyacetophenone to Me_3Al, utilizing the hypervalent property of the Al center.[12] We examined the coordination mode in the complexes of dimethyl maleate and aluminum reagent at RHF and B3LYP levels. Geometry optimization from a structure with two in-plane $COOCH_3$ groups revealed that Me_3Al is coordinated to dimethyl maleate in the monodentate manner. The equilibrium structure has a perpendicular $COOCH_3$ to which the aluminum center coordinates. Although we also examined the structure of a complex with $AlCl_3$, its equilibrium structure was calculated to be the ZZc-I type conformation. These results do not support the proposal by Maruoka et al.

The results concerning the binding energy of the complexes are shown in diagrams (Fig. 10). In Fig. 10, we assumed that the complexation passed through artificial, deformed structures of dimethyl maleate and Lewis acid, of which the structures are the same as those in the complex. Thus, the energy difference between the deformed structures and the equilibrium structures is the deformation energy required by complexation. The energy released by complexation of the deformed dimethyl maleate and Lewis acid is referred to as the interaction energy. The coordination energy is thus decomposed into the deformation energy (positive) and the interaction energy (negative). We must keep in mind two factors about the deformation energy for a certain understanding of this diagram: 1) the energy for conformation changes of dimethyl maleate (E_{DM}) and 2) that of Lewis acid (E_L). Their sum is the deformation energy.

The binding energy of the dimethyl maleate–AlH_2^+ complex is very large (108.3 kcal mol^{-1}). The above scheme gave a deformation energy of 20.4 kcal mol^{-1} (E_{DM} = 9.4 kcal mol^{-1} and E_L = 11.0 kcal mol^{-1}) and an interaction energy of -128.4 kcal mol^{-1}. Apparently, the large negative value of the interaction energy results in the large binding energy. In the case of the maleate–AlH_3 complex, the deformation energy of 6.5 kcal mol^{-1} (E_{DM} = 1.7 kcal mol^{-1} and E_L = 4.8 kcal mol^{-1}) is much smaller than that of the dimethyl maleate–AlH_2^+ complex, because of the smaller structure change. One may expect that this small deformation energy would lead to a large binding energy. However, this is not true; the binding energy of 23.8 kcal mol^{-1} is much smaller than that of the dimethyl maleate–AlH_2^+ complex because of the weak interaction (-30.3 kcal mol^{-1}). Also, the twice amount of this interaction energy is much smaller than the interaction energy in dimethyl maleate–AlH_2^+ (note that the Al atom interacts with two carbonyl oxygen atoms in dimethyl maleate–AlH_2^+, whereas it does so with a single carbonyl oxygen in maleate–AlH_3). This suggests that the electrostatic interaction contributes to the large binding in dimethyl maleate–AlH_2^+.

We have also analyzed the binding energy of dimethyl maleate–$TiCl_4$ complexes. Monodentate and bidentate coordination manners exist in the maleate–$TiCl_4$ complex, and the binding energy of the bidentate complex (8.9 kcal mol^{-1}) is only slightly larger than that of the monodentate complex (6.3 kcal mol^{-1}).

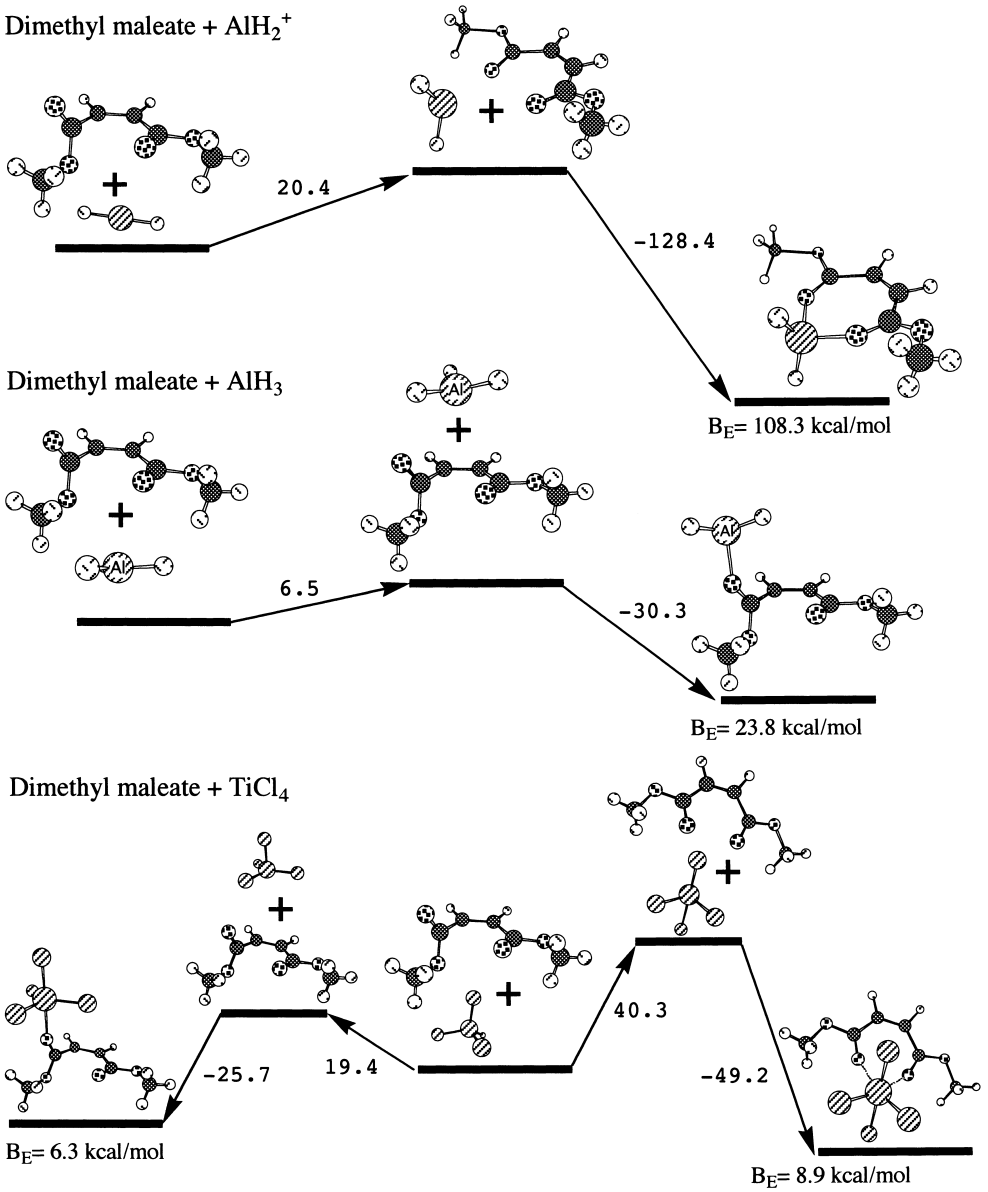

Fig. 10. Energy change during complexation of dimethyl maleate and Lewis acids calculated at the B3LYP/6-31G* levels. Complexation was assumed to pass through deformed dimethyl maleate and Lewis acids, so that in the first step isolated dimethyl maleate and Lewis acids deform and in the second step complexation takes place between them. Energy change of the first step is deformation energy, that of the second step is called interaction energy, and the sum of them corresponds to the binding energy (B_E).

However, the results given in Fig. 10 show that both the deformation and interaction are more significant in the bidentate complex. While the case of the monodentate complex, the deformation energy is 19.4 kcal mol^{-1} (E_{DM} and E_L are 5.6 and 13.8 kcal mol^{-1}, respectively) and the interaction energy is -25.7 kcal mol^{-1}, in the case of the bidentate complex they are 40.3 (E_{DM} = 9.9 kcal mol^{-1} and E_L = 30.4 kcal mol^{-1}) and -49.2 kcal mol^{-1}, respectively. One can notice that in the bidentate complex the deformation of $TiCl_4$, giving the unstable butterfly structure, requires a larger deformation energy. Though the butterfly structure is unstable, it is appropriate for bidentate coordination. Concerning the interaction energy, that of the bidentate complex (-49.2 kcal mol^{-1}) is nearly twice as large as that of the monodentate complex (-25.7 kcal mol^{-1}).

From the above results we can mention that the interaction energy in a monodentate complex is -25 to -30 kcal mol^{-1} and that in a bidentate complex it is twice as large. If an additional factor such as an electrostatic interaction exists, the interaction energy would increase more, as seen for dimethyl maleate–AlH_2^+.

Conclusion

The present study revealed that dimethyl maleate has a peculiarity in equilibrium structures; one of the O=C–O planes is nearly perpendicular to the C–C=C–C plane. It seems reasonable to suppose that the –CH=CH–$COOCH_3$ moiety in dimethyl maleate behaves almost independently from the –$COOCH_3$

moiety. The peculiarity in the equilibrium structures is proposed to be an important origin for the unique properties of maleate. The conformation of the maleate moiety was maintained in the complexes of maleate and a monodentate Lewis acid, such as $AlCl_3$. Bidentate complexation is possible only if two (or more) coordination sites are available on a Lewis acid. $TiCl_4$ and $SnCl_4$ are such a case. We also analyzed the binding energies for those complexes by decomposing them into the deformation energy and the interaction energy. The interaction energy in a monodentate complex is -25 to -30 kcal mol^{-1}, and that in a bidentate complex is twice as large. An additional electrostatic interaction would increase the interaction energy. Calculations of the reactions concerning these equilibrium structures are in progress in order to clarify the reasons for the peculiarities of the reactivity of dialkyl maleates.

Computational Methods

Theoretical calculations were performed using the Gaussian 94 and 98 programs,[13,14] initially at the restricted Hartree–Fock (RHF) level with the 6-31G* basis set. Subsequently, gradient-corrected density functional theory (DFT) with Becke's three-parameter exchange with the Lee, Yang, and Parr correlation functional (B3LYP),[15] were carried out using the 6-31G* basis set. Fourth-order Møller-Plesset perturbation theory (MP4)[16] was used to confirm the relative energy difference of methyl acrylate. For the Sn atom we used the Wadt-Hay effective core potential with double zeta basis functions[17] with an additional d polarization function (the exponent is 0.183). After satisfactory geometry optimization, the vibrational spectrum of each species was calculated.

NK was supported by a Grant-in-Aid on the priority area from the Ministry of Education, Culture, Sports, Science and Technology. Part of the calculations was carried out at the Research Center for Computational Science, Okazaki National Research Institutes.

References

1 a) I. Nanu and C. Andei, *J. Polym. Sci., Polym. Chem. Ed.*, **12**, 231 (1974). b) F. M. Lewis and F. R. Mayo, *J. Am. Chem. Soc.*, **70**, 1533 (1948). c) T. Otsu, O. Ito, N. Toyoda, *J. Macromol. Sci, Chem.*, **A19**, 27 (1983). d) M. Kurokawa and Y. Minoura, *Makromol. Chem.*, **181**, 293 (1980). e) K Urushida, A. Matsumoto, and M. Oiwa, *J. Polym. Sci., Polym. Chem. Ed.*, **19**, 245 (1981).

2 M. Ohno and M. Otsuka, *Org. React.*, **37**, 1 (1989).

3 K. Maruoka, M. Akakura, S. Saito, T. Ooi, and H. Yamamoto, *J. Am. Chem. Soc.*, **116**, 6153 (1994).

4 M. Akakura, K. Maruoka, and H. Yamamoto, unpublished results

5 Y. G. Shtyrlin, D.G. Murzin, N. A. Luzanova, G. G. Iskhakov, and V. D. Kiselev, *Tetrahedron*, **54**, 2631 (1998).

6 a) T. Otsu and N. Toyoda, *Makromol. Chem., Rapid Commun.*, **2**, 79 (1981). b) N. Toyoda, M. Yoshida and T. Otsu, *Poly. J.*, **15**, 255 (1983). c) T. Otsu and K. Shiraishi, *Macromolecules*, **18**, 1795 (1985). d) M. Yoshioka, A. Matsumoto, and T. Otsu, *Macromolecules*, **25**, 2837 (1992).

7 A. Hermann, F. Trautner, K. Gholivand, S. von Ahesen, E. L. Varetti, C. O. Della Vedova, H. Willner, and H. Oberhammer, *Inorg. Chem.*, **40**, 3979 (2001).

8 J. D. Evanseck, K. N. Houk, J. M. Briggs, and W. L. Jorgensen, *J. Am. Chem. Soc.*, **116**, 10630 (1994).

9 a) L. E. Bretscher, C. L. Jenkins, K. M. Taylor, M. L. DeRider, and R. T. Raines, *J. Am. Chem. Soc.*, **123**, 777 (2001). b) E. M. S. Macoas, R. Fausto, J. Lundell, M. Pettersson, L. Khriachtchev, and M. Räsänen, *J. Phys. Chem.*, **105**, 3922 (2001). c) R. D. Bach, O. Dmitrenko, and M. N. Glukhovtsev, *J. Am. Chem. Soc.*, **123**, 7137 (2001).

10 a) M. Dulce, G. Faria, J. J. C. Teixeira-Dias, and R. Fausto, *Vib. Spectrosc.*, **2**, 43 (1991). b) T. Egawa, S. Maekawa, H. Fujiwara, H. Takeuchi, and S. Konaka, *J. Mol. Struct.*, **1995**, 193.

11 a) S. Shambayati and S. L. Schreiber, in "Comprehensive Organic Chemistry," ed by B. M. Trost and I. Fleming, Pergamon, Oxford (1991), Vol. 1, pp. 283–324. b) K. Narasaka, *Synthesis*, **1991**, 1. c) M. Santelli and J.-M. Pons, in "Lewis acids and Selectivity in Organic Synthesis," ed by M. Santelli and J.-M. Pons, CRC Press, Boca Raton (1996), pp.1–20.

12 D. Uraguchi, T. Ooi, and K. Maruoka, *J. Synth. Org. Chem., Jpn.*, **58**, 16 (2000).

13 B. G. Frisch, G. W. Trucks, H. B. Schlegel, P. M. W. Gill, B. G. Johnson, M. A. Robb, J. R. Cheeseman, T. Keith, G. A. Petersson, J. A. Montgomery, K. Raghavachari, M. A. Al-Laham, V. G. Zakrzewski, J. V. Ortiz, J. B. Foresman, J. Cioslowski, B. B. Stefanov, A. Nanayakkara, M. Challacombe, C. Y. Peng, P. Y. Ayala, W. Chen, M. W. Wong, J. L. Andres, E. S. Replogle, R. Gomperts, R. L. Martin, D. J. Fox, J. S. Binkley, D. J. Defrees, J. Baker, J. J. P. Stewart, M. Head-Gordon, C. Gonzalez, and J. A. Pople, "Gaussian 94," Gaussian, Inc., Pittsburgh, PA (1994).

14 B. G. Frisch, G. W. Trucks, H. B. Schlegel, G. E. Scuseria, M.A. Robb, J. R. Cheeseman, V. G. Zakrzewski, J. A., Jr. Montgomery, R. E. Stratmann, J. C. Burant, S. Dapprich, J. M. Millam, A. D. Daniels, K. N. Kudin, M. C. Strain, O. Farkas, J. Tomasi, V. Barone, M. Cossi, R. Cammi, B. Mennucci, C. Pomelli, C. Adamo, S. Clifford, J. Ochterski, G. A. Petersson, P. Y. Ayala, Q. Cui, K. Morokuma, D. K. Malick, A. D. Rabuck, K. Raghavachari, J. B. Foresman, J. Cioslowski, J. V. Ortiz, B. B. Stefanov, G. Liu, A. Liashenko, P. Piskorz, I. Komaromi, R. Gomperts, R. L. Martin, D. J. Fox, T. Keith, M. A. Al-Laham, C. Y. Peng, A. Nanayakkara, C. Gonzalez, M. Challacombe, P. M. W. Gill, B. G. Johnson, W. Chen, M. W. Wong, J. L. Andres, M. Head-Gordon, E. S. Replogle, and J. A. Pople, "Gaussian 98," Gaussian Inc., Pittsburgh, PA (1998).

15 a) A. D. Becke, *J. Chem. Phys.*, **96**, 5648 (1993). b) P. J. Stevens, J. F. Devlin, C. F. Chablowski, and M. J. Frisch, *J. Phys. Chem.*, **98**, 11623 (1994).

16 a) C. Møller and M. S. Plesset, *Phys. Rev.*, **46**, 618 (1934). b) R. Krishnan and J. A. Pople, *Int. J. Quant. Chem.*, **14**, 91 (1978). c) R. Krishnan, M. J. Frisch and J. A. Pople, *J. Chem. Phys.*, **72**, 4244 (1980).

17 a) T. H. Dunning and P. J. Hay, in "Modern Theoretical Chemistry," ed by H. F. Schaefer, III, Plenum, New York (1976), Vol. 3, p. 1. b) P. J. Hay and W. R. Wadt, *J. Chem. Phys.*, **82**, 270 (1985). c) W. R. Wadt and P. J. Hay, *J. Chem. Phys.*, **82**, 284 (1985). d) P. J. Hay and W. R. Wadt, *J. Chem. Phys.*, **82**, 299 (1985).